Supplementary figure legends

Suppl. Fig. S1. ^{1}H-^{15}N HSQC spectra of wild type RelE in the RelB$_C$-free and bound states. The wild type RelE was co-expressed with antitoxin RelB and purified under denaturing conditions. The spectra of a refolded ^{15}N –labeled wild type RelE in free (blue) and RelB$_C$-bound (red) states were recorded under the same conditions as that of the RelE$^{R81A/R83A}$ mutant (Fig. 2). Due to the spectral similarity, assignments of some wild type peaks can be transferred from the RelE$^{R81A/R83A}$ spectrum.

Suppl. Fig. S2. RelB$_C$ binding affinities of wild type RelE and RelE$^{R81A/R83A}$ mutant. Intrinsic tryptophan fluorescence spectra of A, wild type RelE and B, RelE$^{R81A/R83A}$ mutant were recorded as a function of RelB$_C$ concentration. The fluorescence emission spectra were monitored at 20 °C in a wavelength range of 300-400 nm with a fixed excitation wavelength at 295 nm. The sample solution contains 200 nM wild type RelE or RelE$^{R81A/R83A}$ mutant in 20 mM NaPi, 500 mM NaCl, 1 mM DTT and increasing concentration of RelB$_C$ peptide (0-500 nM). The fluorescence emission maximum intensities were plotted against the concentration of RelB$_C$ peptide (insert panels). The dissociation constants (K_D) were fitted using the Hill equation: $F_{obs} = F_0 + F_{max}*S^n/(K_D{}^n + S^n)$, where F_{obs} represents the measured intrinsic tryptophan fluorescence, F_0 and F_{max} represent the minimum and maximum fluorescence values, S represents the peptide concentration and n represents cooperativity coefficient.

Suppl. Fig. S3. Binding induced folding of RelB$_C$ and unfolding of RelE$^{R81A/R83A}$. The chemical shift index (CSI) analysis of A, free (blue) and B, RelE$^{R81A/R83A}$-bound (red) RelB$_C$ reveals a disordered-to-ordered conformational transition upon binding. The CSI analysis of C, free (blue) and D, RelB$_C$-bound (red) RelE$^{R81A/R83A}$ shows the unfolding of the C-terminal helix α4 upon RelB$_C$ binding.

Suppl. Fig. S4. Chemical shift changes mapped on the structure of RelE$^{R81A/R83A}$:RelB$_C$. Two views of the RelE$^{R81A/R83A}$:RelB$_C$ complex rotated by 180 degrees. The solvent accessible surface of RelE$^{R81A/R83A}$ and the ribbon representation of RelB$_C$ are colored with a gradient corresponding to the chemical shift changes associated with their interactions.

Suppl. Fig. S5. Internal motions and dymanics of RelE$^{R81A/R83A}$ affected by RelB$_C$. The ^{1}H-^{15}N heteronuclear NOE analysis of A, free (blue) and B, RelB$_C$-bound (red) RelE$^{R81A/R83A}$. The transverse relaxation rate (R_2) analysis of C, free (blue) and D, RelB$_C$-bound (red) RelE$^{R81A/R83A}$. The relaxation data were recorded in a 800 MHz magnetic field.

Suppl. Fig. S6. Comparison of RelE, aRelE, YoeB and RNase SA structures in complex with their inhibitors. A, The *E. coli* RelE in complex with RelB$_C$ (K47-L79). B, The *P. horikoshii* aRelE with aRelB. C, The *E. coli* YoeB with YefM. D, RNase SA with barstar. The secondary structure elements are colored in navy (helices) and green (strands) for the toxins and RNase; and in magenta (helices) and yellow (strands) for the inhibitors. For clarity, only part of structure of barstar, which directly involves the interaction of YefM, is shown in the panel C and D.

Suppl. Table 1. NMR and refinement statistics for $RelE^{R81A/R83A}$ and $RelE^{R81A/R83A}$:$RelB_C$ structures

	$RelE^{R81A/R83A}$	$RelE^{R81A/R83A}$:$RelB_C$
NMR distance and dihedral constraints		
Distance constraints		
Total NOE	2,440	3,341
Intra-residue	619	801
Inter-residue	1,821	2,192
Sequential ($\|i-j\|=1$)	550	782
Medium-range ($1<\|i-j\|\leq 4$)	481	720
Long-range ($\|i-j\|\geq 5$)	790	690
Intermolecular	0	348
Hydrogen bonds	40 x 2	51 x 2
Total dihedral angle restraints		
ϕ	62	77
ψ	62	77
Structure statistics		
Violations (mean and s.d.)		
Distance constraints (> 0.3 Å)	0 ± 0	1 ± 0
Dihedral angle constraints (> 5º)	0 ± 0	0 ± 0
Max. dihedral angle violation (º)	3.84	2.59
Max. distance constraint violation (Å)	0.248	0.353
Deviations from idealized geometry		
Bond lengths (Å)	0.0097 ± 0.0003	0.0099 ± 0.0003
Bond angles (º)	1.11 ± 0.03	1.18 ± 0.02
Impropers (º)	1.26 ± 0.04	1.41 ± 0.07
Ramachanfran Statistics (%)		
Most favored regions	91.6	85.9
Additionally allowed regions	7.8	13.1
Generously allowed regions	0.4	0.8
Disallowed regions	0.2	0.2
Average pairwise r.m.s. deviation* (Å)		
Heavy (all residues)	1.61 ± 0.16	3.37 ± 0.71
Backbone (all residues)	0.95 ± 0.17	2.73 ± 0.78
Heavy (Ordered region**)	1.31 ± 0.15	1.26 ± 0.12
Backbone (Ordered region)	0.68 ± 0.16	0.54 ± 0.08

* Pairwise r.m.s. deviation was calculated among 20 refined structures. ** Ordered secondary structure components were defined as: F4-F7 (β1), E9-R16 (α1), S20-V33 (α2), E40-N42 (α3), C50-K54 (β2), R61-I67 (β3) and V71-G79 (β4) for both free and bound $RelE^{R81A/R83A}$; E85-R93 (α4) for free $RelE^{R81A/R83A}$; E54-R65 (α3*) and V72-V74 (β2*) for bound $RelB_C$.

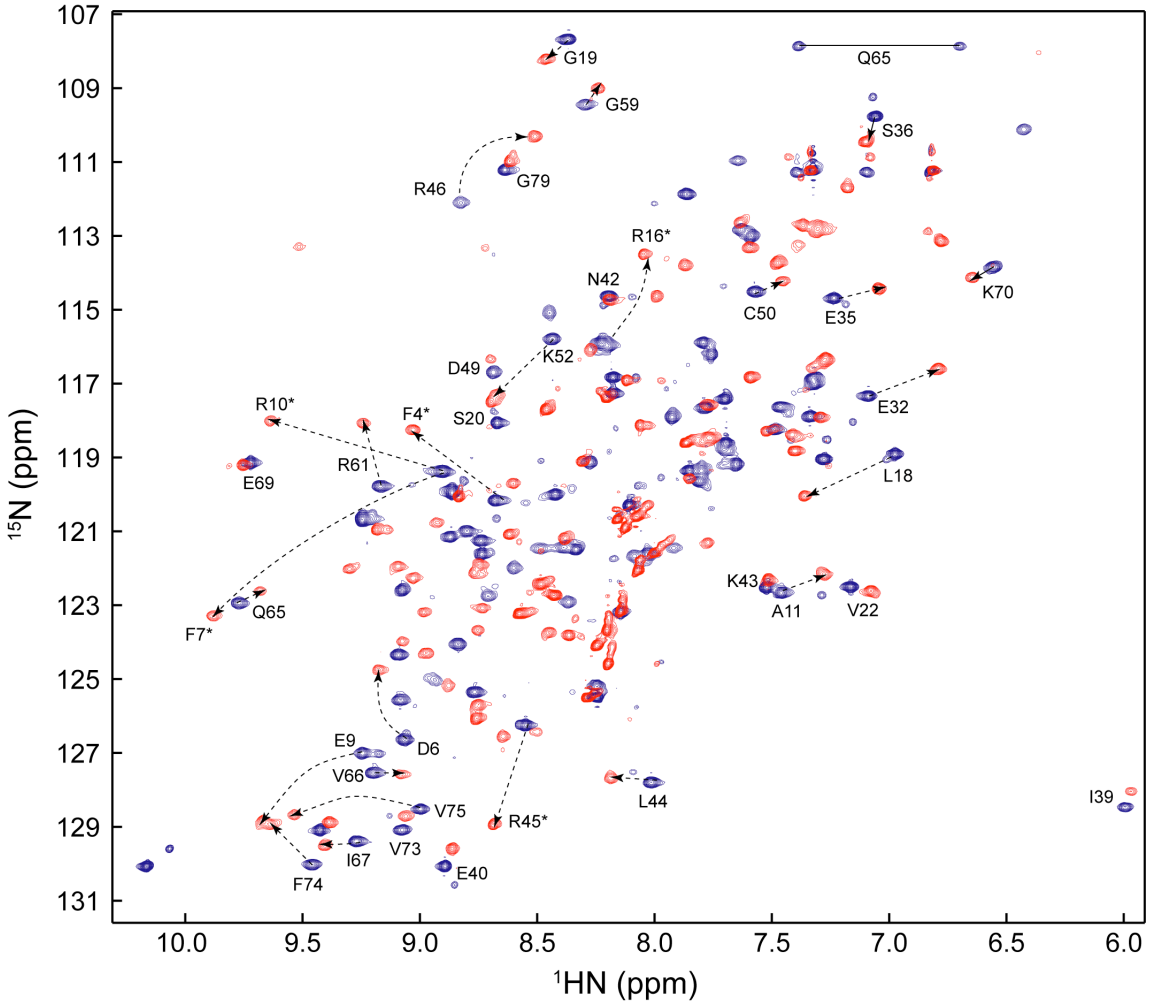
107
109
111
113
115
117
119
121
123
125
127
129
131
^{15}N (ppm)
10.0
9.5
9.0
8.5
8.0
7.5
7.0
6.5
6.0
^{1}HN (ppm)
G19
Q65
G59
S36
R46
G79
R16*
N42
K70
C50
E35
K52
D49
E32
R10*
F4*
S20
R61
E69
L18
K43
A11
V22
F7*
Q65
D6
E9
V66
L44
I39
V75
R45*
I67
V73
F74
E40

Suppl. Fig. S1

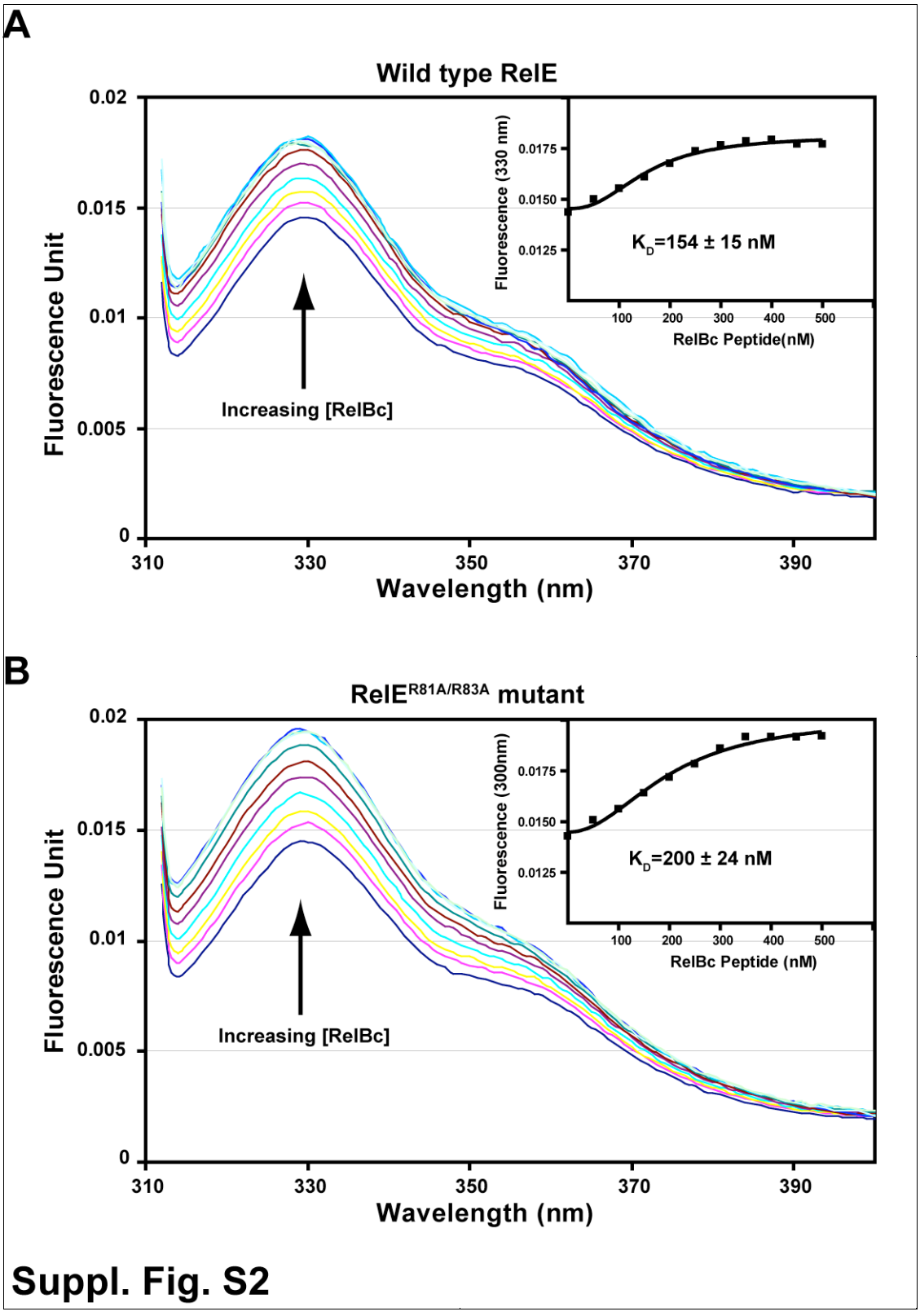
A
Wild type RelE
Fluorescence Unit
Wavelength (nm)
Increasing [RelBc]
Fluorescence (330 nm)
K_D=154 ± 15 nM
RelBc Peptide(nM)
B
RelE^R81A/R83A mutant
Fluorescence Unit
Wavelength (nm)
Increasing [RelBc]
Fluorescence (300nm)
K_D=200 ± 24 nM
RelBc Peptide (nM)

Suppl. Fig. S2

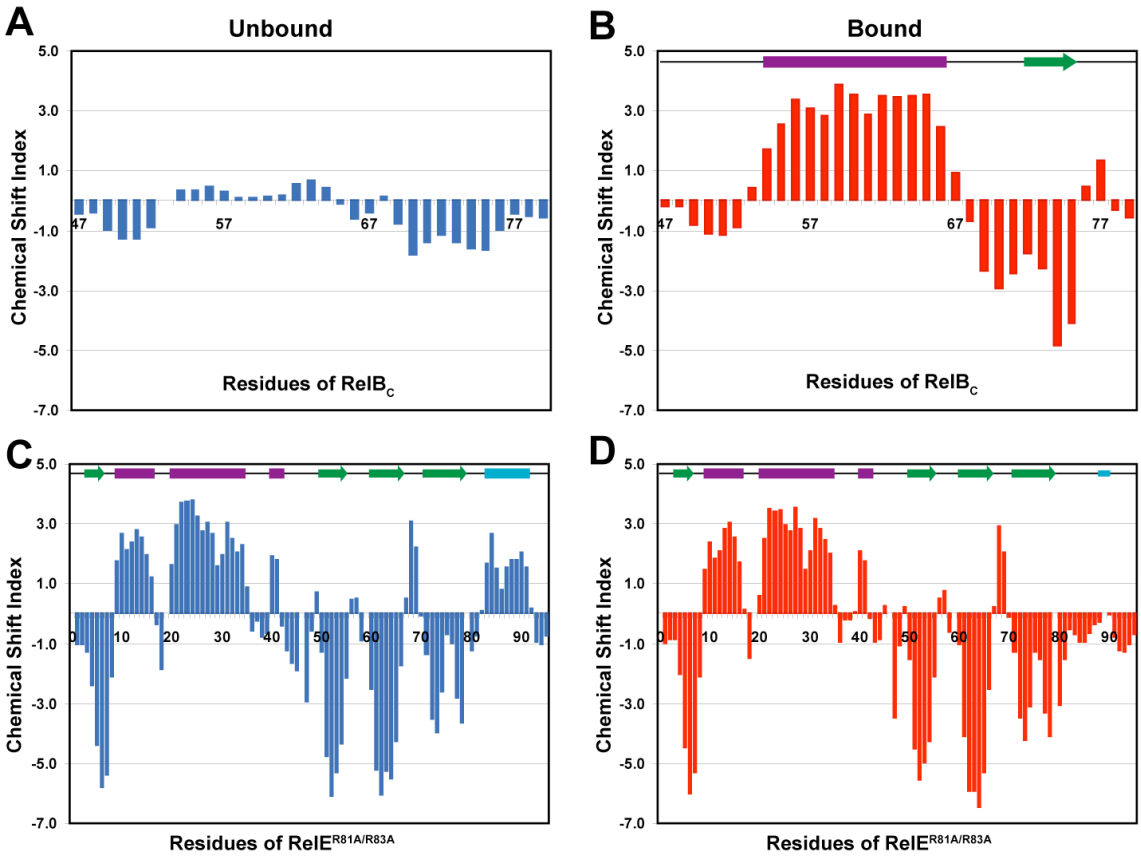
A
Unbound
B
Bound
Chemical Shift Index
5.0
3.0
1.0
-1.0
-3.0
-5.0
-7.0
47
57
67
77
Residues of RelB$_C$
C
D
10
20
30
40
50
60
70
80
90
Residues of RelE$^{R81A/R83A}$

Suppl. Fig. S3

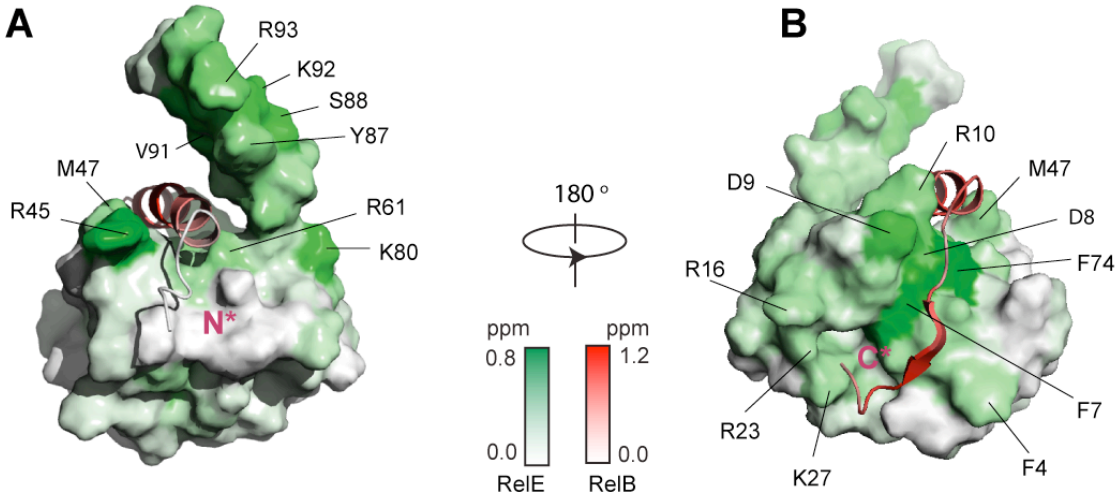
A
R93
K92
S88
Y87
V91
M47
R45
R61
K80
N*
180 °
ppm
0.8
0.0
RelE
ppm
1.2
0.0
RelB
B
R10
M47
D9
D8
R16
F74
C*
F7
R23
K27
F4

Suppl. Fig. S4

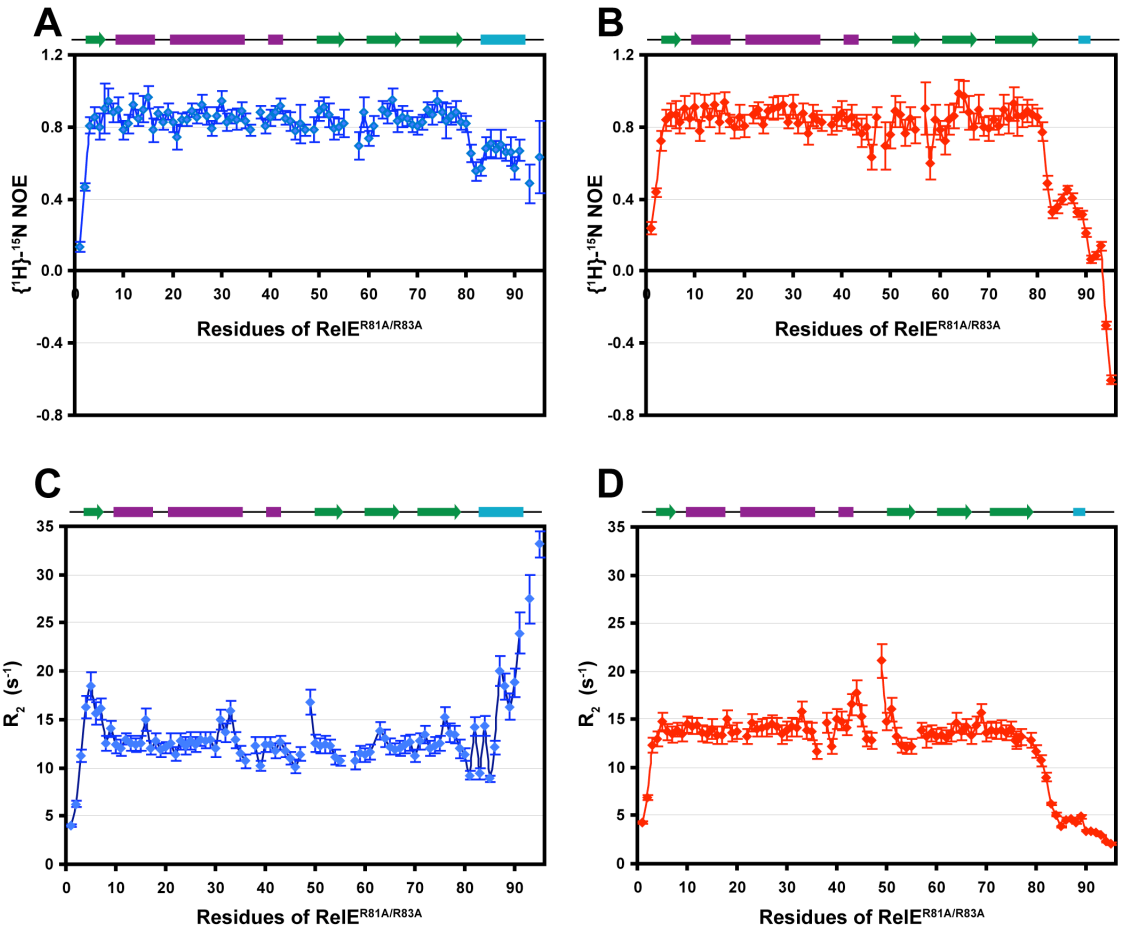

Suppl. Fig. S5

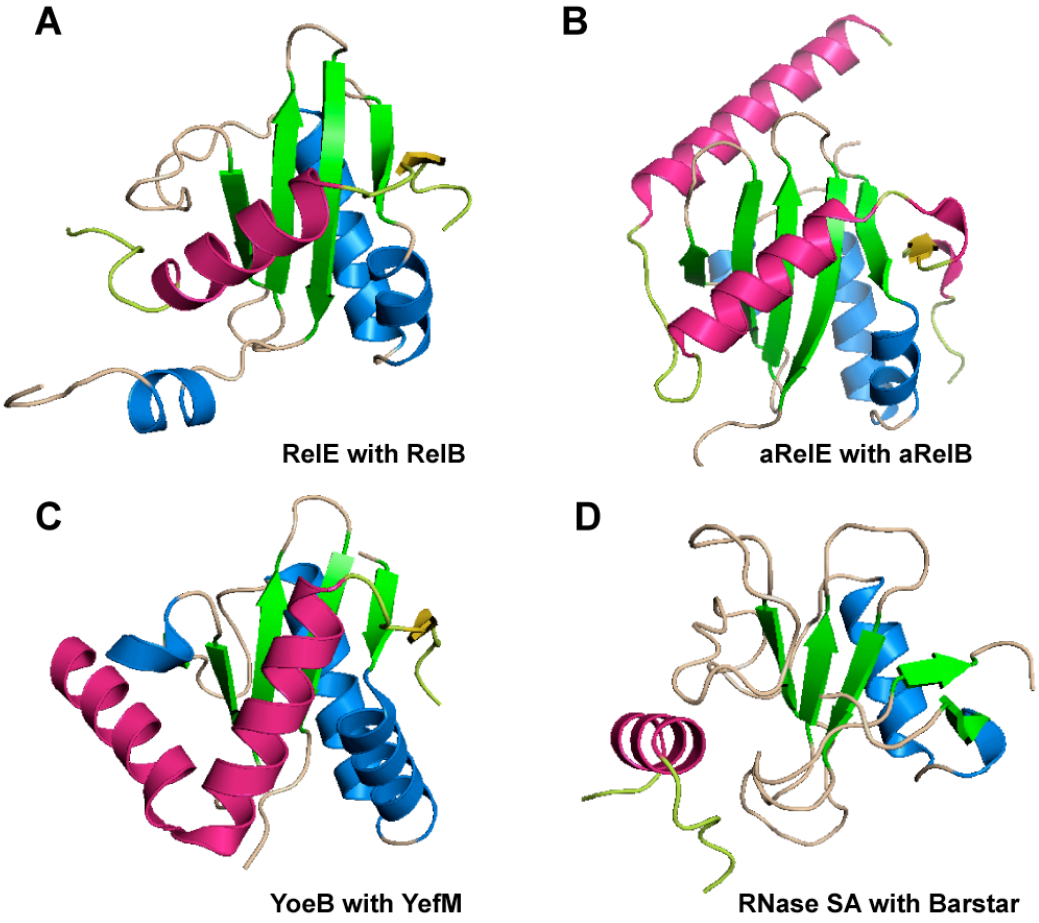
A
RelE with RelB
B
aRelE with aRelB
C
YoeB with YefM
D
RNase SA with Barstar

Suppl. Fig. S6